American Mineralogist, Volume 79, pages 1135–1144, 1994

CO_2-rich glass, round calcite crystals, and no liquid immiscibility in the system CaO-SiO_2-CO_2 at 2.5 GPa

Woh-Jer Lee, Peter J. Wyllie, George R. Rossman
Division of Geological and Planetary Sciences, California Institute of Technology, Pasadena, California 91125, U.S.A.

Abstract

Following reports that the miscibility gap between silicate and carbonate liquids located experimentally on feldspar-calcite joins extended to the alkali-free side of the system CaO-Na_2O-Al_2O_3-SiO_2-CO_2, the melting of a mixture of calcite (70 wt%) and quartz was investigated at 2.5 GPa. The isobaric reaction, calcite (CC) + quartz (Qz) = liquid (L) + vapor (V), was reversed at 1350 °C. Quartz and rounded calcite crystals were concentrated at the bottom of the capsule, and CO_2 was distributed in large vapor bubbles in the glass layer and at the top of the capsule. The liquid quenched to transparent glass, which is unusual in carbonate-rich systems. In two-stage reversal experiments, a sample of L + V that was heated to the subsolidus temperature of 1300 °C produced a few rounded calcite grains organized in dendritic patterns; at 1200 °C, dendritic intergrowths of CC + Qz were produced with some coarser-grained areas. The glass was found to contain about 20 wt% CO_2 on the basis of the geometry of phase boundaries and EDS analysis. There was no evidence for immiscible liquids. The round calcite crystals are equilibrium mineral phases, not quenched $CaCO_3$ liquids, and surface tension effects control their shapes. Infrared spectroscopic studies indicated that $(CO_3)^{2-}$ is the dominant CO_2 species in the glass, and the silicate structure is partially polymerized, probably as a result of interaction between Ca^{2+} and SiO_4 tetrahedra. The phase relationships in the $CaCO_3$-SiO_2 system, the simplest model for subducted oceanic crust with limestone (or for basalt altered by sea water), show that subducted crust potentially could transport calcite to great depths for long-term storage in the mantle and could also yield low-SiO_2 carbonate-rich magmas under some thermal conditions. Such carbonate-rich melts may be efficient agents for mantle metasomatism.

Introduction

Melting relations in silicate-carbonate systems involving carbonate-rich melts are relevant for problems related to mantle metasomatism (Green and Wallace, 1988; Baker and Wyllie, 1992; Yaxley et al., 1991; Hauri et al., 1993), the possible involvement of carbonate-rich melts above subducted oceanic slabs (Sweeney et al., 1992; McInnes and Wyllie, 1992), and the generation of carbonatites and associated volcanism (Bell, 1989). The simplest petrologically relevant system combining silicate and carbonate liquids is CaO-SiO_2-CO_2. Melting relationships in this system (with and without H_2O) have been studied at crustal and mantle pressures (Wyllie and Haas, 1965, 1966; Boettcher and Wyllie, 1969; Huang and Wyllie, 1974; Huang et al., 1980).

Liquid immiscibility occurs between silicates and carbonates, extending across a wide range of compositions (Koster van Groos and Wyllie, 1966, 1973; Koster van Groos, 1975; Freestone and Hamilton, 1980), but there are also continuous liquidus paths between some silicate and carbonate-rich melts (Wyllie, 1989; Otto and Wyllie, 1993). There is excellent petrological and experimental evidence that some carbonatites separated from silicate magmas by liquid immiscibility (Le Bas, 1977; Kjarsgaard and Peterson, 1991; Macdonald et al., 1993), but the limits for the intervention of liquid immiscibility have not been completely determined (Lee and Wyllie, 1992a).

Kjarsgaard and Hamilton (1988, 1989) and Brooker and Hamilton (1990) reported miscibility gaps in several feldspar-carbonate systems at 0.2 and 0.5 GPa between 1100 and 1250 °C, and at 1.5 GPa and 1225 °C, mostly in the presence of CO_2 vapor. Kjarsgaard and Hamilton (1989) presented a generalized projection of miscibility gaps from all their systems into the triangle (Al_2O_3 + SiO_2)-CaO-Na_2O, as shown in Figure 1. Their miscibility gap at 0.5 GPa and 1250 °C extends into alkali-free silicate-carbonate systems, with nearly pure $CaCO_3$ as the end-member immiscible carbonate liquid. Brooker and Hamilton (1990) added a second immiscible carbonate-rich liquid to this arrangement. Remarkably rounded, almost-pure $CaCO_3$ phases were interpreted as quenched, immiscible, carbonate liquid. The occurrence of almost-pure $CaCO_3$ as an immiscible liquid at temperatures several hundred degrees below the fusion temperature of calcite (Irving and Wyllie, 1975) is puzzling. According to these results, a miscibility gap might be expected in the joins $CaCO_3$-SiO_2, $CaCO_3$-$CaSiO_3$, and $CaCO_3$-grossu-

0003–004X/94/1112–1135$02.00

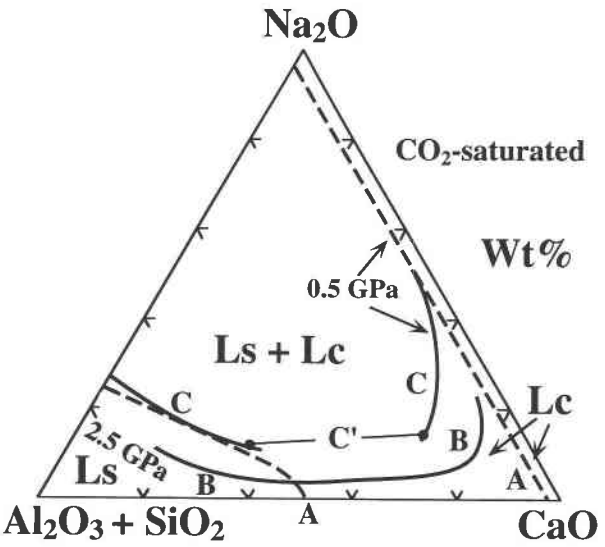

Fig. 1. Silicate-carbonate two-liquid fields projected onto the compositional triangle (Al_2O_3 + SiO_2)-CaO-Na_2O, CO_2-saturated, showing results (heavy curves) from (A) Kjarsgaard and Hamilton (1988, 1989) at 0.5 GPa and 1250 °C, (B) Lee and Wyllie (1992a, and in preparation) at 2.5 GPa, and (C) Kjarsgaard and Hamilton (in preparation) at 0.5 GPa and 1250 °C, presented in Macdonald et al. (1993, Fig. 5b). The tie line C' connects coexisting silicate-rich liquid (Ls) and carbonate-rich liquid (Lc). Note that for A the field Ls + Lc extends all the way to the Na_2O-free side.

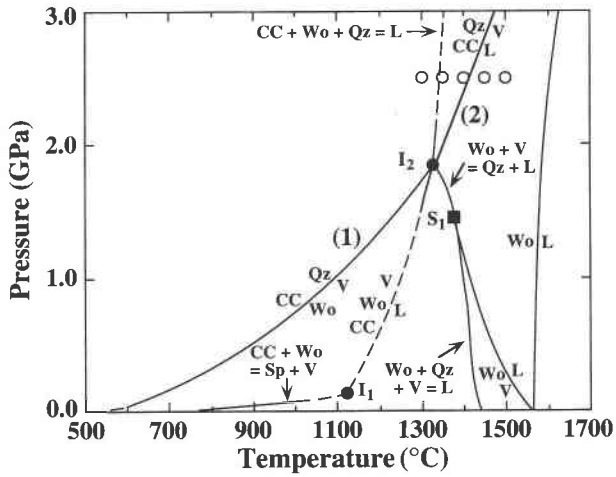

Fig. 2. Selected phase relationships in CaO-SiO_2-CO_2 showing calcite-quartz reactions (Fig. 4 in Huang et al., 1980). Abbreviations: CC = calcite; Wo = wollastonite; Qz = quartz; Sp = spurrite; L = liquid; V = vapor; I = invariant point; S = singular point. The positions of new experiments at 2.5 GPa (Table 1) are given by open circles. Reactions specified in the text are denoted by numbers 1 and 2.

larite previously investigated by Huang et al. (1980), Huang and Wyllie (1974), and Maaloe and Wyllie (1975) at higher pressures (up to 3 GPa). No immiscible liquids were found in these earlier studies, although rounded calcite grains were reported. Lee and Wyllie (1992a, 1992b, and in preparation) studied the phase fields intersected by the join $NaAlSi_3O_8$-$CaCO_3$ at high pressures. The phase relationships required that the rounded $CaCO_3$ phase represent solid calcite under conditions of the experiments, and Lee and Wyllie defined the miscibility gap at 2.5 GPa, as shown in Figure 1. Note that the conjugate Ca carbonate liquid boundary is quite far removed from pure $CaCO_3$.

Macdonald et al. (1993) compared the original 0.5-GPa miscibility gap of Kjarsgaard and Hamilton (1989) with a revised version (Kjarsgaard and Hamilton, in preparation), which is similar to our result at 2.5 GPa (Fig. 1). According to Kjarsgaard (1994 personal communication), the revision involves textural reinterpretation; he is now satisfied that the rounded, almost-pure $CaCO_3$ globules previously interpreted as immiscible liquids are indeed solid calcite under experimental conditions.

In this contribution, we present experiments in the end-member system of Figure 1 to check how the results of Huang et al. (1980) compare with the results of Kjarsgaard and Hamilton (1988, 1989) and Brooker and Hamilton (1990). The original studies of Huang and Wyllie (1974) and Huang et al. (1980) in the system CaO-SiO_2-CO_2 at pressures up to 3 GPa relied on optical examination of crushed fragments in immersion oils and powder X-ray diffraction measurements for the identification of phases. Physical evidence for immiscible liquids was sought on the basis of criteria established by previous experience (e.g., Koster van Groos and Wyllie, 1966, 1973). Glassy beads were present above the solidus, but evidence overall was interpreted in terms of simple liquidus surfaces, without miscibility gaps in the range of compositions studied. Given the recent results cited above, however, reexamination of this boundary system is necessary, using the improvements in textural visualization and interpretation offered by the scanning electron microscope (SEM). The previously reported liquids that quenched to glasses with up to 20 wt% dissolved CO_2 have now been studied by infrared spectroscopic methods (FTIR). Our new results at 2.5 GPa are consistent with the revised 0.5-GPa results in Figure 1 (Kjarsgaard, 1994 personal communication).

Phase relationships in CaO-SiO_2-CO_2: Previous studies

Subsolidus reactions in this system have received much attention (Harker and Tuttle, 1956; Tuttle and Harker, 1957; Haselton et al., 1978). Huang et al. (1980) published a detailed *P-T* projection for the system to 3 GPa, combining their new melting results with all relevant published data, including a tabulation of the experimental data for the phase diagram for $CaSiO_3$-$CaCO_3$ of Huang and Wyllie (1974). Our experiments were conducted on a quartz + calcite mixture. Selected univariant curves emphasizing reactions involving calcite and quartz are

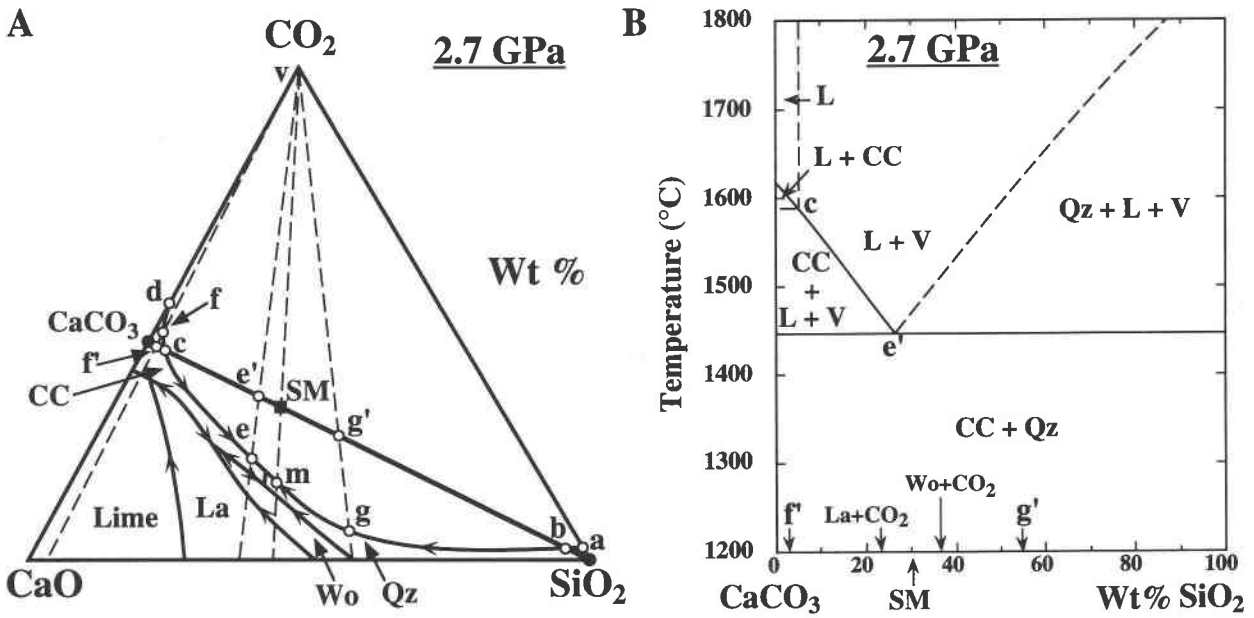

Fig. 3. Phase relationships in CaO-SiO_2-CO_2 at 2.7 GPa from Huang et al. (1980). Abbreviations are as in Fig. 2, and La = larnite. Starting mixture used in this study = SM. (**A**) Vapor-absent liquidus surface extending from CaO to the CO_2-saturated liquidus field boundary a-b-g-m-e-c-f-d, giving liquid compositions coexisting with vapor, v. Liquid e is involved in Reaction 2: CC + Qz = L + V. (**B**) Phase fields intersected by the join $CaCO_3$-SiO_2. Compare c, e', and SM in **A** and **B**.

reproduced in Figure 2. Calcite and quartz dissociate together in the reaction

$$\text{calcite} + \text{quartz} = \text{wollastonite} + \text{vapor} \qquad (1)$$

(Harker and Tuttle, 1956, to 0.3 GPa) at pressures up to the invariant point I_2 at 1.85 GPa and 1325 °C (Huang et al., 1980), where the assemblage is joined by liquid. Haselton et al. (1978) studied several subsolidus decarbonation reactions and derived f_{CO_2} data from the results. Their curve for Reaction 1 is somewhat higher than that in Figure 2 at lower pressures, but within error limits it passes through point I_2. Among the array of curves emanating from I_2, the incongruent melting reaction

$$\text{calcite} + \text{quartz} = \text{liquid (e)} + \text{vapor (v)} \qquad (2)$$

rises to higher pressure. The phase relationships and Reaction 2 are illustrated in Figure 3.

Figure 3A shows the phase compositions in the ternary reactions at 2.7 GPa, with liquid field-boundary compositions constrained by the several joins studied by Huang et al. (1980). The curve a-b-e-c-d is the vapor-saturated liquidus boundary, giving liquid compositions coexisting with minerals and almost-pure CO_2 vapor at v. The field boundaries divide the CO_2-undersaturated liquidus surface into areas for the primary precipitation of calcite, quartz, wollastonite, larnite, and lime. Reaction 2, like Reaction 1, is a dissociation reaction, and the liquid compositions formed from mixtures on the join $CaCO_3$-SiO_2 between b and c have lost CO_2. Figure 3B shows the phase fields intersected by the join $CaCO_3$-SiO_2 at 2.7 GPa, according to Huang et al. (1980). The eutectic-like liquid e' in Figure 3B is a projection of the ternary liquid e, as shown in Figure 3A.

Kjarsgaard and Hamilton (1989) did not claim that immiscible liquids exist between quartz or calcium silicates and calcite, but a literal interpretation of their original results in Figure 1, and those of Brooker and Hamilton (1990), implies a miscibility gap between about f' and g' on the line CC-Qz in Figure 3A and 3B, which corresponds to the interval f and g on the field boundary a-d in Figure 3A. [This is no longer required by Kjarsgaard's reinterpretation (in preparation); Fig. 1.]

Experimental methods

Primary standard-grade $CaCO_3$ powders (Alfa Products) and reagent-grade SiO_2 powders (Puratronic) were dried at 110 °C for at least 1 d. A mixture of 30 wt% quartz and 70 wt% calcite was ground under ethanol in an agate mortar to obtain a fine-grained, uniform mixture. About 5 mg of the mixture for each experiment was dried for >1 h in a vacuum drying oven at 110 °C before being loaded into Pt capsules about 4 mm long. This starting bulk composition is identified in Figure 3 by SM.

Experiments were done in a piston-cylinder apparatus 1.27 cm in diameter, with calcium fluoride as a pressure medium. Temperature was controlled and monitored by $W_{95}Rh_5$-$W_{74}Rh_{26}$ thermocouple, with no correction for the effects of pressure on the emf. Experiment duration varied from 0.5 to 4 h, depending on the temperature. Experiments were terminated by turning off the electrical power. The quenching rate was about 100 °C/s for the first 600 °C, and it dropped to about 50 °C/s or less at

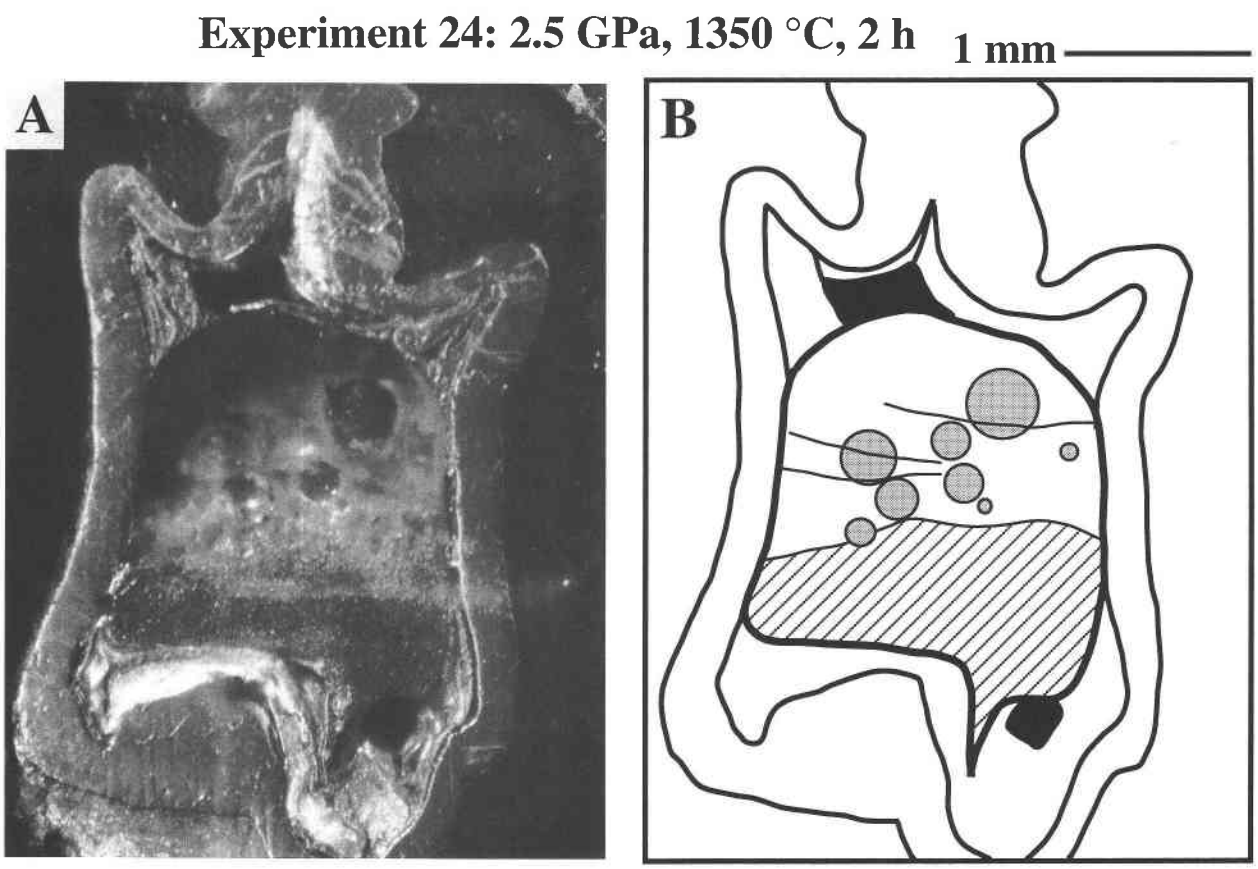

Fig. 4. Polished sample from expt. no. 24: 2.5 GPa, 1350 °C, 2 h (Table 1). (A) Photograph of the Pt capsule, sliced open and polished. (B) Sketch identifying the phases. Diagonal shading = calcite and quartz; white area above is clear glass; gray circles and black areas contained vapor during the experiment.

lower temperatures. Pressure was not held constant during quenching. The pressure accuracy is about ±0.05 GPa, and temperature accuracy is estimated to be ±10 °C, according to many previous calibrations with this furnace assembly.

Polished surfaces of experimental products were analyzed with a Camscan scanning electron microscope fitted with an energy-dispersive system (EDS). Quenched liquids and crystals were analyzed using a beam current of 0.1 nA on brass with 15 kV acceleration voltage. The quenched liquids were analyzed in raster modes, with a covered area of about 100 μm^2. The identification of phases was based on texture and morphology observed with a petrographic microscope (with both reflected and transmitted light) and SEM, and compositions were determined by EDS. A thin, plane-parallel plate of glass from the sample of experiment 151, prepared by polishing both sides, was used in a spectroscopic study to identify the CO_2 species in glass and to obtain quantitative analyses utilizing infrared absorption spectra from a Nicolet 60SX FTIR spectrometer. In addition, a polished surface of the sample in experiment 151 was prepared to obtain the infrared reflectance spectra with a Nicolet Nic-Plan IR microscope.

Experimental results

The starting mixture was selected to be near the projected eutectic e′ in Figure 3, just within the field for liquidus quartz. The criteria for identifying Reaction 2 are (1) the appearance of liquid, (2) the disappearance of calcite, (3) the appearance of a vapor phase, and (4) probably an increase in the size of quartz compared with the subsolidus assemblage. Few melting reactions in silicate-carbonate systems have been satisfactorily reversed because the liquid commonly crystallizes to a dendritic aggregate during normal rapid quench, and this texture is retained during subsolidus annealing. Therefore, it has been difficult to reach unambiguous conclusions about whether the texture in a reversal experiment was formed during the quench or during the experiment at temperature below the solidus. Because the liquid in our experiments quenched to a glass, we were able to study textures of minerals grown from liquid during annealing in two-stage reversal experiments.

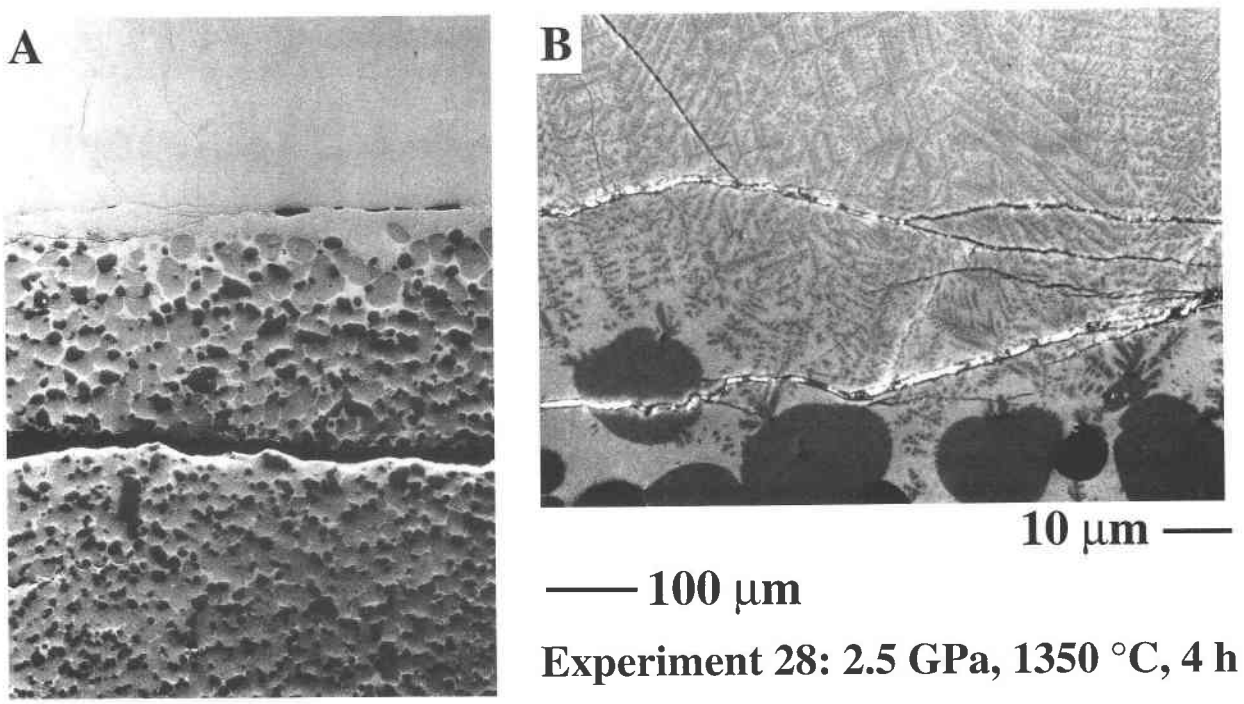

Fig. 5. SEM photomicrograph of expt. no. 28: 2.5 GPa, 1350 °C, 4 h (Table 1)—the result is similar to that illustrated in Fig. 4—spanning the boundary between crystals and glass. (**A**) Low magnification. The rounded calcite crystals are medium gray, and the smaller quartz crystals are darker gray. The amount of the interstitial glass (lightest gray) decreases with distance below the boundary. (**B**) High magnification. Calcite dendrites are in the glassy area near the boundary between glass and crystals. The medium gray, rounded crystals at the bottom are calcite, and the dark gray, subrounded crystals are quartz.

Experiments are listed in Table 1, and their positions are shown in Figure 2. Experimental products are illustrated in Figures 4, 5, and 6, and the results for experiments of various duration (0.5–4 h) are plotted in Figure 7. For comparison, experiments by Huang et al. (1980) on this join at 2.7 GPa varied from 30 to 40 min.

Phase relationships

Figure 4 illustrates an experiment with all phases present (expt. 24, Fig. 7A). The top part of the sample consists of clear glass enclosing large vapor bubbles, with additional vapor cavities above the glass. The lower part consists of crystals of calcite and quartz, with interstitial glass. The corresponding experiment of longer duration (expt. 28) contains the same assemblages, with the sharp interface between the two parts shown in the SEM microphotographs (Fig. 5A). There are fine dendrites extending about 200 μm into glass from the interface between glass and the crystal layer (Fig. 5B), presumably resulting from nucleation during the quench on calcite crystals. The small percentage of glass between the crystals decreases with distance below the interface. The rounded calcite grains in contact with liquid reported by Huang et al. (1980) are clearly displayed. Quartz grains vary from subangular to rounded.

The short-duration experiment at 1400 °C (expt. 23) produced the same four-phase assemblage with similar phase distribution, but the 2-h experiment (no. 26, Fig. 7A) was essentially L + V, with traces of calcite and quartz remaining at the bottom of the capsule. The experiment at 1300 °C (no. 27) is similar to the lower portion of Figures 4 and 5, but with only a trace of interstitial liquid (estimated 1%), distributed sporadically, and small vapor pits along the boundaries among crystals and liquid. At constant pressure, the four-phase assemblage should be isothermal, so we conclude that Reaction 2 occurs at 1350 °C and attribute the trace of liquid at lower temperature to a trace of absorbed H_2O in the starting material. Calcite formed with polyhedral morphology in contact with other calcite grains, but in the presence of interstitial liquid it became subrounded.

The results of three reversal experiments are shown in Figure 7B. Experiments 34R and 41R were first held at 1500 °C for 0.5 h to produce liquid and vapor (Fig. 7A), and temperatures were then rapidly lowered into the subsolidus region at 1300 and 1200 °C, respectively, for 2 h (Fig. 7B). The reversal to 1300 °C consisted largely of glass, with vapor bubbles and some calcite (Fig. 6A), whereas the reversal to 1200 °C contained a much higher proportion of crystals (Fig. 6B). Figure 6A shows sparse,

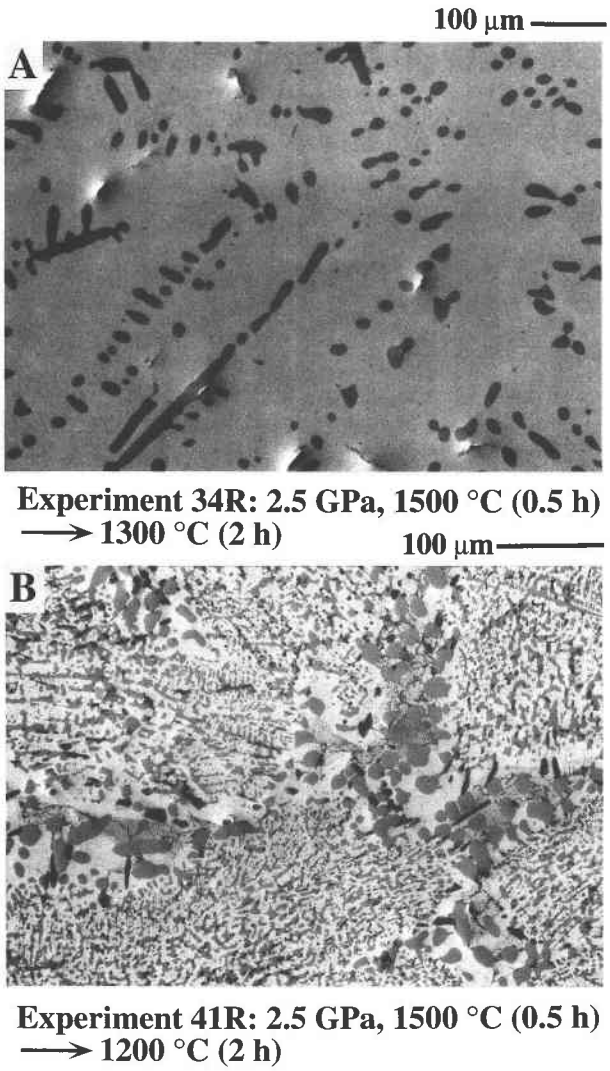

Fig. 6. SEM photomicrographs of experiments reversed from the assemblage L + V at 1500 °C (Table 1). Phases in direction of lighter gray: quartz → calcite → liquid. (**A**) Expt. no. 34R, held at 1300 °C. Glass with calcite dendrites, composed of small rounded units arranged in linear structures. (**B**) Expt. no. 41R, held at 1200 °C. Calcite dendrites and very small quartz grains with interstitial quenched liquid, with glass increasing in amount locally in regions of coarser grain size.

rounded grains to elongated ovoids of calcite with organized structure in dendritic form. A few quartz crystals were found near the edge of the sample. The reversal to 100 °C lower consisted for the most part of glass containing fine-grained dendritic calcite-quartz intergrowths, enclosing some irregular areas with much larger, elongated calcite and a few larger prismatic quartz crystals. Reversal experiment 35R was conducted initially to generate the four-phase assemblage of Figure 4 and then lowered through 50 °C into the subsolidus region. The upper, originally liquid part produced sparse, rounded calcite in dendritic arrays (compare Fig. 6A), the interface between the two parts became less well defined, and a few hexagonal or rounded prismatic crystals of quartz grew in the glass near the interface.

TABLE 1. Experiment results in the system $CaO-SiO_2-CO_2$ at 2.5 GPa for the mixture 70% calcite, 30% quartz

Expt.	T (°C)	t (h)	Resulting assemblage at P and T
21	1500	0.5	L + V
151	1500	0.67	L + V
22	1450	0.5	L + V
23	1400	0.5	L + V + CC + Qz
26	1400	2	L + V + CC (tr) + Qz (tr)
24	1350	2	L + V + CC + Qz
28	1350	4	L + V + CC + Qz
27	1300	2	CC + Qz + L (tr) + V (tr)
34R	1500 to 1300	0.5 to 2	L + V + CC + Qz (tr)
35R	1350 to 1300	2 to 2	L + V + CC + Qz
41R	1500 to 1200	0.5 to 2	L + V + CC + Qz

Note: abbreviations are defined as follows: CC = calcite, Qz = quartz, L = liquid, V = vapor, tr = trace amount. The expt. nos. marked by R indicate reversals. For example, expt. 34R was first held at 1500 °C for 0.5 h and then quenched to 1300 °C and held for 2 h.

Many more experiments would be necessary to work out the detailed nature of mineral nucleation and growth during subsolidus annealing, but these experiments confirm that Reaction 2 is in reversible equilibrium at temperatures near 1350 °C, with results consistent with the topology of the phase diagram in Figure 3B. This temperature is about 50 °C lower than the curve of Huang et al. (1980). Despite the observation that liquids in many carbonate-rich systems cannot be quenched to glasses, the liquid compositions near e (Fig. 3A) crystallize only slowly, even 150 °C below the solidus. For the equilibrium assemblage of calcite + quartz to grow, it is necessary for the free CO_2 to diffuse into the subsolidus glass and to combine with Ca^{2+}, which probably has to be extracted from strong bonding in the SiO_4 structural environment.

Rounded calcite without liquid immiscibility

Kjarsgaard and Hamilton (1988, 1989) and Brooker and Hamilton (1990) have interpreted rounded and dumbbell-shaped calcite grains as liquids with compositions equal to or very close to pure $CaCO_3$, immiscible with the silicate-rich liquid in which they were suspended, but Kjarsgaard (1994 personal communication) is now satisfied with the interpretation of Lee and Wyllie (1992b) that round $CaCO_3$ in the join albite-calcite represents a solid mineral. Although the round calcite in our experiments with liquid certainly has the physical appearance of an immiscible liquid (Fig. 5), we are satisfied that its distribution proves it was a mineral under experimental conditions and not a $CaCO_3$ liquid.

Evidence that the round calcite represents a mineral phase rather than quenched liquid includes the following: (1) the intermixed distribution of round calcite and quartz beneath a layer of silicate liquid (Fig. 5), (2) the restriction of the assemblage (rounded calcite and other phases) to a few tens of degrees between the solidus and a homo-

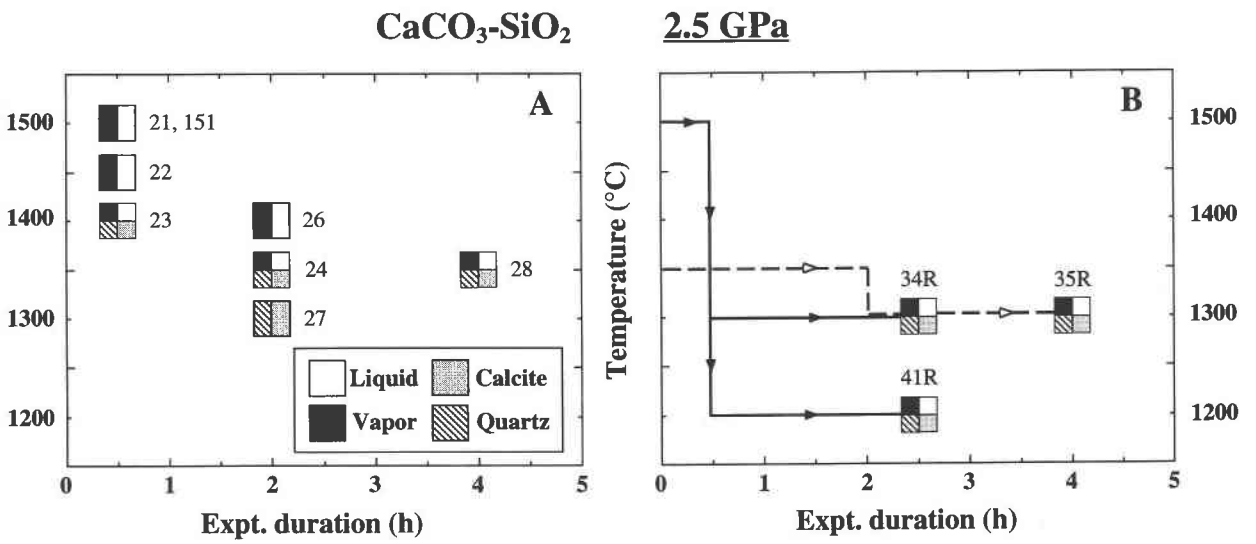

Fig. 7. Experimental results and reversals, showing the effect of time (for experiment numbers, see Table 1, and for experiment positions see Figs. 2 and 3B). (**A**) The 2-h experiments define Reaction 2: CC + Qz = L + V at 1350 ± 50 °C. See Table 1 and text for discussion of the phase assemblages for expt. nos. 26 and 27. (**B**) Two-stage reversal experiments showing temperature and duration of each stage. Expt. nos. 34R and 41R were first held for 0.5 h at 1500 °C, and expt. no. 35R was first held at 1350 °C for 2 h.

geneous silicate-CO_2 liquid, (3) the rounded calcite grains in the experiment reversed from the liquid field being parts of an organized dendritic feature (Fig. 6A), which represents the growth of crystals and not the exsolution of liquid (which subsequently solidified to pure $CaCO_3$), (4) the melting temperature of calcite at 2.7 GPa being 1615 °C (Fig. 3B), which is more than 250 °C higher than the disappearance of the round phase (labeled calcite) in Figure 7, and (5) the internally consistent phase relations by Huang et al. (1980) for the complete system CaO-SiO_2-CO_2 without the intervention of liquid immiscibility, which are now confirmed by our test of the phase fields intersected by the join SiO_2-$CaCO_3$ at 2.5 GPa (Figs. 2 and 3).

The results in Table 1 and Figure 7 and the samples illustrated in Figures 4, 5, and 6 are consistent with the previous interpretation of a simple eutectic reaction, and we cannot see how these results could be reconciled with a miscibility gap in Figure 3B. The same arguments apply to the round calcite grains in the join grossular-$CaCO_3$ at 3.0 GPa (Maaloe and Wyllie, 1975). The rounded shapes of the calcite crystals are most probably the result of surface tension effects between calcite and the carbonate-silicate liquids.

Composition of glass

The composition of the liquid formed from the starting mixture in our experiments was estimated from EDS analyses using SEM, complementing the chemographic solubilities represented by the phase diagram in Figure 3A of Huang et al. (1980). No attempt was made to measure CO_2 solubility by weight loss after ignition or by FTIR.

The ratio of SiO_2 to CaO in the glass from L + V experiments measured by EDS/SEM was coincident with that in the starting mixture SM. The presence of vapor confirmed that the glass composition contained less CO_2 than did SM and therefore lay on the line v-SM extended in Figure 3A. The determination of CO_2 in the quenched glasses using EDS analysis was based on the deficiency of total detectable elements below 100%, using calcite as a reference phase and applying a correction based on quartz analyses. The results (probable error 1–2 wt%) showed decreasing CO_2 solubility with increasing temperature: 1350 °C = 17.0%, 1400 °C = 16.9%, 1450 °C = 15.6%, and 1500 °C = 14.2%. These values straddle m in Figure 3A.

Huang et al. (1980) estimated the position of the CO_2-saturated liquidus field boundary a-b-e-c-d (Fig. 3A) from the geometry of phase fields intersected by several joins through the system. Their field boundary gave a value of about 16 wt% for the CO_2 content of liquid m, which is the liquid composition obtained by projection through v-SM. Complete melting of the mixture SM should yield liquid m and vapor v (compare Fig. 3B).

Structure of glass

The infrared reflectance spectrum of the glass from experiment 151 is illustrated in Figure 8A. It shows a broad band between 1160 and 1570 cm^{-1}, resulting from the ν_3 vibrational mode of the $(CO_3)^{2-}$ unit, which is split into two peaks at 1477 and 1392 cm^{-1}. The peak positioned at 854 cm^{-1} is assigned to the ν_2 vibration of carbonate. Other bands in Figure 8A between 550 and 1160 cm^{-1} are attributed to silicate vibrations. The broad feature between 550 and 800 cm^{-1} is probably due to the Si-O-

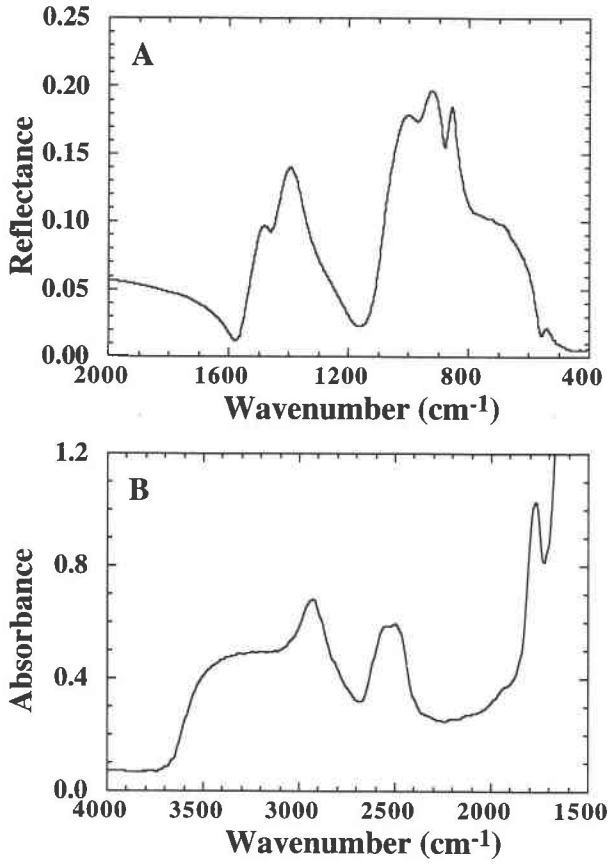

Fig. 8. IR spectra for glass produced from expt. no. 151, 2.5 GPa, 1500 °C, 40 min (Table 1, Fig. 7A). **(A)** Infrared reflectance spectrum from a polished surface of the glass, taken as ratios of reflection intensity of the glass to that of a reference Au surface, illustrating bands from carbonate vibrations around 854 cm^{-1} and between 1160 and 1570 cm^{-1}, and the broad feature for silicate vibrations between 550 and 1160 cm^{-1}. **(B)** Infrared absorption spectrum from a doubly polished slab of the glass 80 μm in thickness, illustrating carbonate bands at 1780, 2520, and 2920 cm^{-1}.

Si asymmetric bending and the bridging O asymmetric stretching vibrations. The features between 800 and 1160 cm^{-1} result from the asymmetric Si-O stretching of SiO_4 tetrahedra. These assignments are summarized in McMillan (1984). The two peaks at 995 and 917 cm^{-1} probably arise from the stretching of silica tetrahedra with two and three nonbridging O atoms, respectively. This gives an indication of partial polymerization in the glass. Figure 8B is an infrared absorption spectrum of the glass quenched from 1500 °C (expt. 151), showing a broad band between 3700 and 2300 cm^{-1}, superimposed with two narrower bands centered at 2520 and 2920 cm^{-1}. The broad band is caused by OH^- stretching (equivalent to about 0.5 wt% total H_2O in the glass, using the calibration of Newman et al., 1986), and the two bands around 2520 and 2920 cm^{-1} are assigned to the combination of the $\nu_1 + \nu_3$ vibrational modes and the first overtone of ν_3 for the $(CO_3)^{2-}$ complex, respectively. The split on the ν_3 mode in Figure 8A is mimicked in the 2520-cm^{-1} band but no longer is resolved in the 2920-cm^{-1} band. The intensity of the characteristic band around 2350 cm^{-1} for the ν_3 antisymmetric stretching mode of molecular CO_2 is insignificant compared with the carbonate bands in the glass spectrum. Therefore, the CO_2 species in the glass is mainly carbonate.

TABLE 2. Comparison of integrated molar absorption coefficients between calcite [$CC_{(0001)}$ and CC_{mean}] and the carbonate-rich silicate glass (QzCC glass)

	$CC_{(0001)}$*	CC_{mean}**	QzCC glass (no. 151)
Density (g/cm³)	2.71		2.79
CO_2 content (wt%)	44.0% (stoichiometry)		13.7% (EDS)
Coefficients at 2500 cm^{-1} [L/(mol·cm²)]	659	316	660 (±30)
Coefficients at 2900 cm^{-1} [L/(mol·cm²)]	625	338	570 (±50)

Note: the uncertainties of the coefficients for the glass were estimated on the basis of the uncertainties on the determination of peak intensity only, whereas the uncertainties of the coefficients for calcite are negligible compared with those for the glass, and therefore they are not listed in this table.

* Coefficients of $CC_{(0001)}$ are calculated values for the (0001) face under unpolarized light based on the measured intensities of bands using a polarized light with *E* perpendicular to the **c** crystallographic axis on a cleavage face.

** Coefficients of CC_{mean} are calculated means over all possible directions of light incident on a calcite crystal, using the expression $CC_{mean} = -\log(10^{-IA/HW} \times 0.75 + 0.25) \times HW$, where IA = integrated absorbance of a band on the (0001) face (calculated) and HW = half width of the band.

The bands at 2520 and 2920 cm^{-1} discussed above may be used for the quantitative analysis of CO_2 concentrations in glasses, but such an analysis requires a detailed calibration for this purpose. Table 2 compares the CO_2 molar absorption coefficients of a calcite crystal with the glass from experiment 151, on the basis of chemical data from EDS/SEM and the IR spectroscopy, with the technique described elsewhere (e.g., Fine and Stolper, 1985). The uncertainty is somewhat large if both the uncertainties on the base-line correction for the peaks (Table 2) and the CO_2 concentration from EDS are considered. However, it indicates that the absorption coefficients of the carbonate bands in the glass are generally higher than those of calcite (CC_{mean}, a calculated mean over all possible orientation of calcite crystals) and likely are due to the greater distortion on the carbonate ions in the glass. The transparent nature of the quenched liquids and the slow growth rate of calcite crystals during both quenching and reversal experiments are likely to be controlled by the liquid structure. However, the detailed effects of liquid structures on the growth mechanism of calcite are not established. Probably the sluggish crystallization is due to the strong interaction of Ca^{2+} with SiO_4 tetrahedra.

DISCUSSION

The main objective of this study was to test for immiscible liquids in the system $CaO-SiO_2-CO_2$, given the

results of Kjarsgaard and Hamilton (1988, 1989) and Brooker and Hamilton (1990) in related systems summarized in Figure 1. Associated objectives were to examine their interpretation of the rounded and dumbbell-shaped $CaCO_3$ phase as a quenched liquid, with the resultant conclusion that the immiscible carbonate liquids could be extremely rich in $CaCO_3$.

No miscibility gap was found between silicate and carbonate liquids at high pressures, which is consistent with the previous conclusion (Huang et al., 1980) and with Kjarsgaard's revised interpretation in related systems at 0.5 GPa (in Macdonald et al., 1993). The rounded calcite crystals shown in Figure 5 illustrate the tendency of calcite to form in rounded habits in many systems, including those without silicates (e.g., Wyllie and Tuttle, 1960). We presented evidence supporting our conclusion (Lee and Wyllie, 1992a, 1992b) that the round $CaCO_3$ phase in quenched samples in parts of the system $Na_2O-CaO-Al_2O_3-SiO_2-CO_2$ represented crystalline calcite under experimental conditions, which is now accepted by Kjarsgaard's reinterpretation (1994 personal communication). This interpretation, along with our results from $NaAlSi_3O_8-CaCO_3$ from 1.0 to 2.5 GPa and Kjarsgaard's revised miscibility gap at 0.5 GPa, indicates that, although immiscible carbonate liquids may be sövitic, they appear to remain well separated from pure $CaCO_3$ in composition.

The occurrence of metasomatism by carbonate-rich melts in mantle lherzolites is now well established (e.g., Yaxley et al., 1991; Hauri et al., 1993; Ionov et al., 1993). These melts may be derived by the action of CO_2 on lherzolite (e.g., Wyllie and Huang, 1976; Eggler, 1978; Wallace and Green, 1988; Dalton and Wood, 1993) or by CO_2 or melts derived from subducted oceanic crust (Huang et al., 1980; Sweeney et al., 1992). The conditions under which partially carbonated oceanic crust might transport carbonate deep into the Earth's interior for long-term storage, or might become reduced to generate diamonds (Luth, 1993), or might yield a carbonate-rich melt are of particular interest.

The two reactions in Figure 2 showing the stability limit of dry pelagic limestones, represented by the assemblage calcite + quartz, are situated well above expected temperatures in subducted oceanic crust, confirming that calcite may survive subduction for storage in the mantle (Huang et al., 1980). In the presence of H_2O, however, reaction and partial melting would yield traces of carbonate-rich melt at much lower temperatures (Wyllie and Haas, 1965; Boettcher and Wyllie, 1969; Huang et al., 1980). The results in Figure 3 focus on the existence of a eutectic, vapor-saturated liquid, with composition near 45% CaO, 35% SiO_2, and 20% CO_2, coexisting with calcite and quartz at 2.5 GPa, and with calcite and wollastonite at pressures below about 1.8 GPa (Fig. 2, Huang et al., 1980). If pockets of pelagic limestones survive subduction, they can generate liquids of this composition at depths of 100 km or more where temperatures reach 1500 °C. Such liquids would change composition rapidly by reaction with lherzolite or eclogite, causing significant metasomatic changes in the host rocks as they changed into the carbonate-rich melts in equilibrium with their more mafic hosts.

The significance of the predominance of $(CO_3)^{2-}$ over molecular CO_2 dissolved in the liquids at 2.5 GPa in the system $CaO-SiO_2-CO_2$, along with the structural information, indicates that up to 20% of carbonates can be incorporated into partially polymerized silicate liquid in the presence of a high content of network modifiers, such as Ca^{2+}. Hence, a CO_2-rich silicate liquid at mantle conditions can evolve to be highly carbonated as silicates are fractionated during magma transportation. The liquid is slow to crystallize, however, compared with most carbonate-rich liquids, which cannot be quenched to glasses. Figure 6A shows the sluggish behavior of liquid carried 50 °C below its solidus temperature, where only a few calcite dendrites have crystallized.

Our partly melted experimental samples demonstrated the ease with which carbonate-rich magma, if formed, could be separated from its source rock (Hunter and McKenzie, 1989; White and Wyllie, 1992). Figure 4 shows a 2-h experiment in which all crystals were concentrated into a lower layer, with only little interstitial liquid remaining. It appears that it takes longer for the large CO_2 vapor bubbles to rise through the liquid than it does for minerals to settle out from the liquid or for liquid to rise from the mineral matrix.

Acknowledgments

This research was supported by the Earth Science section of the U.S. National Science Foundation, with grants EAR-9218806 (P.J.W.) and EAR-9104059 (G.R.R.). This is contribution no. 5412 of the Division of Geological and Planetary Sciences, California Institute of Technology.

References cited

Baker, M.B., and Wyllie, P.J. (1992) High-pressure apatite solubility in carbonate-rich liquids: Implications for mantle metasomatism. Geochimica et Cosmochimica Acta, 56, 3409–3422.

Bell, K., Ed. (1989) Carbonatites: Genesis and evolution, 618 p. Unwin Hyman, London.

Boettcher, A.L., and Wyllie, P.J. (1969) The system $CaO-SiO_2-CO_2-H_2O$: III. Second critical end-point on the melting curve. Geochimica et Cosmochimica Acta, 33, 611–632.

Brooker, R.A., and Hamilton, D.L. (1990) Three-liquid immiscibility and the origin of carbonatites. Nature, 346, 459–462.

Dalton, J.A., and Wood, B.J. (1993) The compositions of primary carbonate melts and their evolution through wallrock reaction in the mantle. Earth and Planetary Science Letters, 119, 511–525.

Eggler, D.H. (1978) The effect of CO_2 upon partial melting of peridotite in the system $Na_2O-CaO-Al_2O_3-MgO-SiO_2-CO_2$ to 35 kbar, with an analysis of melting in a peridotite-H_2O-CO_2 system. American Journal of Science, 278, 305–343.

Fine, G., and Stolper, E. (1985) The speciation of carbon dioxide in sodium aluminosilicate glasses. Contributions to Mineralogy and Petrology, 91, 105–121.

Freestone, I.C., and Hamilton, D.L. (1980) The role of liquid immiscibility in the genesis of carbonatites: An experimental study. Contributions to Mineralogy and Petrology, 73, 105–117.

Green, D.H., and Wallace, M.E. (1988) Mantle metasomatism by ephemeral carbonatite melts. Nature, 336, 459–462.

Harker, R.I., and Tuttle, O.F. (1956) Experimental data on the P_{CO_2}-T

curve for the reaction: Calcite + quartz = wollastonite + carbon dioxide. American Journal of Science, 254, 239–256.

Haselton, H.T., Sharp, W.E., and Newton, R.C. (1978) CO_2 fugacity at high temperatures and pressures from experimental decarbonation reactions. Geophysical Research Letters, 5, 753–756.

Hauri, E.H., Shimizu, N., Dieu, J.J., and Hart, S.R. (1993) Evidence for hotspot-related carbonatite metasomatism in the oceanic upper mantle. Nature, 365, 221–227.

Huang, W.-L., and Wyllie, P.J. (1974) Eutectic between wollastonite II and calcite contrasted with thermal barrier in $MgO-SiO_2-CO_2$ at 30 kbar, with applications to kimberlite-carbonatite petrogenesis. Earth and Planetary Science Letters, 24, 305–310.

Huang, W.-L., Wyllie, P.J., and Nehru, C.E. (1980) Subsolidus and liquidus phase relationships in the system $CaO-SiO_2-CO_2$ to 30 kbar with geological applications. American Mineralogist, 65, 285–301.

Hunter, R.H., and McKenzie, D. (1989) The equilibrium geometry of carbonate melts in rocks of mantle composition. Earth and Planetary Science Letters, 92, 347–356.

Ionov, D.A., Dupuy, C., O'Reilly, S.Y., Kopylova, M.G., and Genshaft, Y.S. (1993) Carbonated peridotite xenoliths from Spitsbergen: Implications for trace element signature of mantle carbonate metasomatism. Earth and Planetary Science Letters, 119, 283–297.

Irving, A.J., and Wyllie, P.J. (1975) Subsolidus and melting relationships for calcite, magnesite, and the join $CaCO_3-MgCO_3$ to 36 kbar. Geochimica et Cosmochimica Acta, 39, 35–53.

Kjarsgaard, B.A., and Hamilton, D.L. (1988) Liquid immiscibility and the origin of alkali-poor carbonatites. Mineralogical Magazine, 52, 43–55.

——— (1989) The genesis of carbonatites by immiscibility. In K. Bell, Ed., Carbonatites: Genesis and evolution, p. 388–404. Unwin Hyman, London.

Kjarsgaard, B.A., and Peterson, T. (1991) Nephelinite-carbonatite liquid immiscibility at Shombole volcano, East Africa: Petrographic and experimental evidence. Mineralogy and Petrology, 43, 293–314.

Koster van Groos, A.F. (1975) The effect of high CO_2 pressures on alkalic rocks and its bearing on the formation of alkalic ultrabasic rocks and the associated carbonatites. American Journal of Science, 275, 163–185.

Koster van Groos, A.F., and Wyllie, P.J. (1966) Liquid immiscibility in the system $Na_2O-Al_2O_3-SiO_2-CO_2$ at pressures to 1 kilobar. American Journal of Science, 264, 234–255.

——— (1973) Liquid immiscibility in the join $NaAlSi_3O_8-CaAl_2Si_2O_8-Na_2CO_3-H_2O$. American Journal of Science, 273, 465–487.

Le Bas, M.J. (1977) Carbonatite-nephelinite volcanism, 347 p. Wiley, London.

Lee, W.-J., and Wyllie, P.J. (1992a) New data on CO_2-rich immiscible liquids in $Na_2O-CaO-Al_2O_3-SiO_2-CO_2$ from 25 to 1 kb: Carbonatite genesis (abs.). Eos, 73 (14), 349–350.

——— (1992b) Liquid immiscibility between silicates and carbonates must intersect suitable liquidus field boundaries to have petrogenetic significance. International Geological Congress, Kyoto, Abstracts, 29, 571.

Luth, R.W. (1993) Diamonds, eclogites, and the oxidation state of the Earth's mantle. Science, 261, 66–68.

Maaloe, S., and Wyllie, P.J. (1975) The join grossularite-calcite through the system $CaO-Al_2O_3-SiO_2-CO_2$ at 30 kilobars: Crystallization range of silicates and carbonates on the liquidus. Earth and Planetary Science Letters, 28, 205–208.

Macdonald, R., Kjarsgaard, B.A., Skilling, I.P., Davies, G.R., Hamilton, D.L., and Black, S. (1993) Liquid immiscibility between trachyte and carbonate in ash flow tuffs from Kenya. Contributions to Mineralogy and Petrology, 114, 276–287.

McInnes, B.I.A., and Wyllie, P.J. (1992) Scapolite formation and the production of nephelinitic melts during the subduction of carbonated basalt (abs.). Eos, 73 (43), 637.

McMillan, P. (1984) A Raman spectroscopic study of glasses in the system $CaO-MgO-SiO_2$. American Mineralogist, 69, 645–659.

Newman, S., Stolper, E.M., and Epstein, S. (1986) Measurement of water in rhyolitic glasses: Calibration of an infrared spectroscopic technique. American Mineralogist, 71, 1527–1541.

Otto, J.W., and Wyllie, P.J. (1993) Relationships between silicate melts and carbonate-precipitating melts in $CaO-MgO-SiO_2-CO_2-H_2O$ at 2 kbar. Mineralogy and Petrology, 48, 343–365.

Sweeney, R.J., Green, D.H., and Sie, S.H. (1992) Trace and minor element partitioning between garnet and amphibole and carbonatitic melt. Earth and Planetary Science Letters, 113, 1–14.

Tuttle, O.F., and Harker, R.I. (1957) Synthesis of spurrite and the reaction wollastonite + calcite = spurrite + carbon dioxide. American Journal of Science, 255, 226–234.

Wallace, M.E., and Green, D.H. (1988) An experimental determination of primary carbonatite magma composition. Nature, 335, 343–346.

White, B.S., and Wyllie, P.J. (1992) Solidus reactions in synthetic lherzolite-H_2O-CO_2 from 20–30 kbar, with applications to melting and metasomatism. Journal of Volcanology and Geothermal Research, 50, 117–130.

Wyllie, P.J. (1989) Origin of carbonatites: Evidence from phase equilibrium studies. In K. Bell, Ed., Carbonatites: Genesis and evolution, p. 500–545. Unwin Hyman, London.

Wyllie, P.J., and Haas, J.L. (1965) The system $CaO-SiO_2-H_2O$: I. Melting relationships with excess vapor at 1 kilobar pressure. Geochimica et Cosmochimica Acta, 29, 871–892.

——— (1966) The system $CaO-SiO_2-CO_2-H_2O$: II. The petrogenetic model. Geochimica et Cosmochimica Acta, 30, 525–544.

Wyllie, P.J., and Huang, W.-L. (1976) Carbonation and melting reactions in the system $CaO-MgO-SiO_2-CO_2$ at mantle pressures with geophysical and petrological applications. Contributions to Mineralogy and Petrology, 54, 79–107.

Wyllie, P.J., and Tuttle, O.F. (1960) The system $CaO-CO_2-H_2O$ and the origin of carbonatites. Journal of Petrology, 1, 1–46.

Yaxley, G.M., Crawford, A.J., and Green, D.H. (1991) Evidence for carbonatite metasomatism in spinel peridotite xenoliths from western Victoria, Australia. Earth and Planetary Science Letters, 107, 305–317.

Manuscript received December 23, 1993
Manuscript accepted July 11, 1994